TEMPERATURES BEHAVIOURE OF SOME ALLOY STEELS IN TURNING PROCESS UNDER DIFFERENT OPRATING CONDITIONS.

Asmaa A. kawi
Department of Mechanical Engineering,
College of Engineer
University of Basrah /Basrah/Iraq

ABSTRACT

Based on three-dimension transient heat diffusion equation a FEM model was developed to simulate coupled thermo-mechanical deformation effects on temperature behavior for four alloys steel during turning process . Alloys used as a workpiece were AISI 1045, AISI 1030, AISI 4340 and AISI 4140, parameters such as cutting speed, feed rate were changed to explore their effect on temperature behavior. The results show that Finite element method is a successful technique to perform analysis to estimate cutting temperatures, a possibility of developing temperature forms adequately representing metal cutting temperature as a Polynomial models of third, fourth and fifth degree with time that give steady state temperature and for the four alloys steel used and different operation conditions. All alloys have a sever increasing temperature with increasing feed rate, while it looks less sharp with increasing cutting speed .Also the ratio of the number of nodes have maximum temperature for any operating conditions and any alloy used with respect to the total number of nodes is less than 1%.

KEYWORDS: Turning process, Alloys Steel, Steady state Temperature, Work-piece Temperature, FEM

سلوك درجات الحرارة لبعض سبائك الفولاد في عمليه الخراطه ولظروف عمل مختلفه

اسماء عاصي كاوي

قسم الهندسه الميكانيكيه/كليه الهندسه

جامعه البصره / البصره / العراق

الخلاصه

استنادا إلى معادلةِ انتقال الحرارةِ 3D لحالة عدم الاستقرار و باستخدام تقنية العناصر المحددة طوّر نمــــودج لمحاكــاة تاتيراتِ التشوه الميكانيكي – الحراري المزدوج على سلوكِ درجةِ الحرارة لاربعة سبائك من الفولاد خلال عمليــة الخراطــه. السبائك المستخدمة في هذا البحث كانت AISI 4340 ,AISI1030 ,AISI 1045 و AISI 4140 . اخدت قيم مختلفة لكــل من سرعة القطع ومعدل التغذية لمعرفة تاثيرهما على سلوك درجة الحرارة في السبائك المدروسة. بينت النتائج نجاح تقنيـــة العناصر المحددة في حساب درجات الحرارة . إمكانية استخراج معادلات ملائمة لتمثل درجة حرارة القطع كمتعددة حدود من الدرجة الثالثة والرابعة و الخامسة مع الزمن لإيجاد درجة حرارة القطع بعد الوصول للاستقرار للسبائك الاربعة ولشروط عمل مختلفه. كل السبائك المدروسه تمتلك زيادة حادة في درجه حرارة القطع مع ازدياد معدل التغذيه في حين تبدو هده الزياده اقل

حِده مع زيادة سرعه القطع. نسبِهِ عددِ العقدِ التي لها درجه حرارة فصوى لايَ حاله تشغيل واي سبيكه نسبه الى العددِ الكلــــي للعقدِ تكون اقل مِنَ   %.

SAMPLE	
A	Initial Yield Strength of the Material at Room Temperature and a Strain rate of 1/sec
B,C,D,E ,m and n	dimensionless constant for each material
c_p	Heat Capacity
f	Feed Rate
f_s	Frictional Stress
h	Heat Convection Coefficient
k	Thermal Conductivity
p	Interface Pressure between two Bodies
q	Heat Loss due to Free Convection
T	Temperature
T , T_{melt}	Room and Melt Temperatures
t1	Depth of Cut
V	Cutting Speed
	Density
	Material Parameter
σ	Flow Stress
$\dot{\varepsilon}$	Strain

NOMECLATURE

$\bar{\dot{\varepsilon}}$	Strain Rate
$\bar{\dot{\varepsilon}}$	Reference Strain Rate

INTRODUCTION

   Metal cutting operations still represent the largest class of manufacturing operations where turning is the most commonly employed material removal process (Karpat). Alloy steels are pronounced as difficult to cut materials and this can be hardened by regular process (**Derakhshan, 2009**).Turning of these types of alloys require a knowledge of coupled deformation and thermal turning simulation of work piece. Intelligent design of tool and other process parameters is a key factor for effective processing (to get proper dimensions, internal deformation and microstructure distribution) and ensuring that the required product properties are achieved according to customer specifications.

    Due to more demanding manufacturing systems, the requirements for reliable technological information have increased. This calls for a reliable analysis in the cutting zone (Tool–work piece–chip system) (**Haci Saglam, 2006**). Metals cutting are associated with high temperatures and hence the thermal aspects of the cutting process strongly affect the accuracy of the machining process. The high temperatures generated in the deformation zones have serious consequences for both the tool and the work-piece. Cutting temperatures strongly influence tool wear, tool life, work-piece surface integrity, chip formation mechanism and contribute to the thermal deformation of the cutting tool (**Abukhshim,2005**) and (**Rogério,2009**). The chip formation process in machining is accompanied by heat generation, which influences the mechanical and physical properties of both the work-piece and the cutting tool (Vincent and others, 2004). The unique tribological contact phenomenon, which occur in metal cutting is non-linear, and occurs at high temperatures, high pressures and high strains. This has made it extremely difficult to predict in a precise manner or even assess the

performance of various models developed for modeling the machining process. An accurate and repeatable heat and temperature prediction remains challenging due to the complexity of the contact phenomena in the cutting process. Measuring temperature and the prediction of heat distribution in metal cutting is extremely difficult due to a narrow shear band, chip obstacles, and the nature of the contact phenomena where the two bodies, tool and chip, are in continuous contact and moving with respect to each other (**Abukhshim, 2006**).

Therefore, numerous attempts have been made to approach this problem with different methods including experimental, analytical and numerical analysis using different workpiece materials specially alloy steel. A model to analyze the heat transfer and temperature distribution in rotary tool turning of hardened 52100 steel (58 HRC) was developed based on the moving heat source theory of conduction and employs the finite element method (FEM) for its solution (Vincent and others, 2004). A comparison study between the measured and calculated results of cutting force components and temperature variation generated on the tool tip in turning for different cutting parameters and different tools having various tool geometries while machining AISI 1040 steel hardened at HRc 40 (**Haci ,2006**). A low carbon steel (C15) and a low alloyed medium carbon steel (42CrMo4) was machined experimentally and the performances of the measurement setup are completed by the possibility of recording real time photographs of the chip formation (**Sutter, 2007**). These records make the analysis of temperature maps easier and allow specific parameters as the contact length at the tool-chip interface or the shear angle to be determined. The effects of insert design in turning of steel parts and surface finishing has been investigated in finish turning of AISI 1045 steel using conventional and wiper design inserts (**Özel ,2009**). Regression models and neural network models were developed for predicting surface roughness, mean force and cutting power.

 A computational model to determine the temperature distribution in a metal cutting process based on multi-dimensional steady state heat diffusion equation along with heat losses by convection film coefficients at the surfaces was studied using the finite element method (**Pradip, 2005**). Results were presented for the machining of high-speed carbon steel and for a range of cutting conditions. An estimation of the amount of heat flowing into the cutting tool in high speed turning of AISI/SAE-4140 was achieved experimentally (**Abukhshim, 2005**). The aim is to characterize the thermal field in the cutting zone and thus understand the mechanics of high speed machining. Prediction of heat generation, heat partition and temperature distribution in metal machining includes an exploration of the different simplifying assumptions related to the geometry of the process components, material properties, boundary conditions and heat partition was studied theoretically and experimentally (**Abukhshim, 2006**). The work presented the results of extensive cutting tests performed to measure temperature along the tool-chip interface line when machining BS 970-709M40EN19 (AISI/SAE-4140) high strength alloy steel. The thermal problems in dry orthogonal turning devoted to C45 medium carbon steel with natural contact tools treated with multi-layer coatings with an intermediate Al2O3 layer (**Grzesik, 2006**). New hybrid analytical models for estimating heat partition to the chip and the tool–chip interface temperatures were proposed to estimate the average and maximum steady-state tool–chip interface temperatures in orthogonal turning. Modeling of the tool temperature distribution was addressed in self-propelled rotary tool (SPRT) machining of hardened steels (**Vincent, 2004**). This model was developed to analyze the heat transfer and temperature distribution in rotary tool turning of hardened 52100 steel (58 HRC). The model is based on the moving heat source theory of conduction and employs the finite element method (FEM) for its solution. A moving heat source along the surface of a half space was used to simulate the turning operation (**Jing, 2005**). 3D square source problems are solved numerically by using finite element analysis. The surface temperature distribution inside and outside the contact area and the temperature distribution in the medium are obtained.

Most of the efforts in studying heat transfer have been directed toward determining temperature distributions in the chip and tool. In contrast, little attention was focused on the direct evaluation of the heat transfer process in the work-piece, either experimentally or theoretically. Furthermore, mechanical properties of the work-piece such as tensile strength, work-piece surface integrity and hardness need to be correlated with microstructural parameters which effected in a sharp by work-

piece temperature. In this study a finite element computational model to determine temperature distribution in the work-piece, tool and chip in turning process was developed. The model is based on 3D unsteady state heat diffusion equation along with heat losses by convection coefficients at the surfaces. Four different alloy steel were machined by using one kind of tool inserts, under various operating conditions.

A parametric study will be carried out to investigate the effect of operating conditions on the temperature rise distribution, maximum and steady state temperature of the work-piece.

THERMAL PHENOMENA IN SIMULATION OF MECHANICS OF 3D TURNING

Turning is a very important machining process in which a single point cutting tool removes unwanted material from the surface of a rotating cylindrical work piece. The cutting tool is fed linearly in a direction parallel to the axis of rotation. three cutting parameters namely cutting speed(V) , feed rate(f) and depth of cut(t_1) need to be optimized in a turning operation (**Abhang, 2010**),as shown in **Fig(1-a)**. Analysis of the thermal fields in turning process has been the topic of research interest for many years. It is a complex problem, involving many parameters and is too cumbersome to be truly simulated in any mathematical form (**Sarat, 2005**). The main regions where heat is generated during the orthogonal cutting process are shown in **Fig. (1-b)**, Firstly, heat is generated in the primary deformation zone due to plastic work done at the shear plane. The local heating in this zone results in very high temperatures, thus softening the material and allowing greater deformation. Secondly, heat is generated in the secondary deformation zone due to work done in deforming the chip and in overcoming the sliding friction at the tool-chip interface zone. Finally, the heat generated in the tertiary deformation zone, at the tool work-piece interface, is due to the work done to overcome friction, which occurs at the rubbing contact between the tool flank face and the newly machined surface of the work-piece. Heat generation and temperatures in the primary and secondary zones are highly dependent on the cutting conditions (**Abukhshim, 2006**). While for the tertiary region that depending on the friction modelling, which required an accurate model definition.

The amount of heat generate in the work-piece resulting in a highly localized thermo mechanically coupled deformation in the shear zone. Temperatures in the cutting zone considerably affect the stress–strain relationship, fracture and the flow of the work-piece material. Generally, increasing temperature decreases the strength of the work-piece material and thus increases its ductility. It is now assumed that nearly all of the work done by the tool and the energy input during the machining process are converted into heat (**Abukhshim, 2006**).

PROBLEM FORMULATION AND BOUNDARY CONDITIONS

The tool geometry and the cutting conditions used for the orthogonal metal cutting simulation are presented in **Table 1**. During the cutting process, force exerted by the tool is converted into heat at a contact area between the tool edge and the chip which diffuses throughout the cutting tool and work-piece by conduction process according to the heat transfer equation for a three dimensional problem for unsteady state:

$$(\rho c_p) \, \partial T/ \partial t = k (\partial^2 T/ \partial x^2 + \partial^2 T/ \partial y^2 + \partial^2 T/ \partial z^2) \tag{1}$$

where k is the thermal conductivity , T temperature, t time, ρ density ,c_p heat capacity x perpendicular length , y the moving direction of the tool and z is the depth of work-piece.

Machining is performed at ambient temperature assuming the initial temperature of whole model at room temperature, T(x, y, z, t)= T(x, y, z, 0)=20°C .The exterior boundaries of the tool-work-piece are exposed to the air; except at the tool–chip contact area, which are exposed to the environment, heat loss due to convection (h=20 W/m² °C) is considered as shown in **Fig.2** where the elements marked in green are affected by free convection.

$$q=h (T-T_\infty) \tag{2}$$

The far end surface of the tool holder and work-piece, which are distant from the cutting zone, is assumed to be at room temperature (T =20 ˚C). In contact area the frictional law is usually based on the Coulomb model, Eq. (3), with a constant friction coefficient, these laws are often modified with more realistic models, in which a constant shear model, Eq. (4), is used to describe the phenomenon close to the tool tip (sticking zone), while a Coulomb model properly fits in the complementary area of the contact length (sliding zone) (**DEFORM-3D User manual, 2007**).

$$f_s = m \qquad\qquad\qquad\qquad\qquad (3)$$
$$f_s = \mu p \qquad\qquad\qquad\qquad\qquad (4)$$

where f_s is the frictional stress, m is the friction factor,   is the shear yield stress, μ is the friction factor and p is the interface pressure between two bodies .

The bottom surface of the work-piece is fixed in all directions. The cutting tool is modeled as a rigid body which moves at the specified cutting speed. Tungsten carbide (WC) insert was used in this study as the cutting tool.

The material-constitutive laws often include the effect of strain (rigid–plastic or elastic–plastic), strain rate (rigid–viscoplastic or elastic–viscoplastic) and temperature (thermal softening). DEFORM 3D uses Oxley's equation, Eq. (5), which used to express the flow stress relation and Johnson–Cook law, Eq. (6) (**DEFORM-3D manual, 2007**). Eqs (5) and (6) are linking the flow stress to the strain, strain rate and temperature, are the most popular and widely used to develop numerical models of the cutting process and represent the material flow stress behavior under the machining condition in this study. Unfortunately, for only a few low carbon steels is such a documented relationship available. For high carbon content steel or their hardened products, such as AISI H13 steel and (hardened) 52100 bearing steel, there are no such available documented constitutive equations that are required as the inputs for Oxley's predictive machining theory ,for that we chose this four alloy in this work.

$$\overline{\sigma} = \overline{\sigma}(\dot{\varepsilon}, \dot{\overline{\varepsilon}}, T) \qquad\qquad\qquad\qquad (5)$$

$$\overline{\sigma} = (A + B\overline{\varepsilon}^n)[1 + C\ln(\frac{\dot{\overline{\varepsilon}}}{\dot{\varepsilon}_\circ})][\frac{\dot{\overline{\varepsilon}}}{\dot{\varepsilon}_\circ}]^\alpha \{D - ET^{*m}\} \qquad (6)$$

Where $T^* = (\dfrac{T - T_{room}}{T_{melt} - T_{room}})$

the constant A is in fact the initial yield strength of the material at room temperature and a strain rate of 1/sec and   represents the plastic equivalent strain. Temperature term in the J-C model reduces the flow stress to zero at the melting temperature of the work material $\overline{\sigma}$ is the flow stress, $\dot{\varepsilon}$ is the strain, $\overline{\varepsilon}$ is the strain rate and T is temperature. Parameters of the Johnson–Cook equation (C, D, E, m, and n are dimensionless constant for each material).The thermal conductivity, heat capacity and thermal expansion properties for alloys chosen are changing with temperature. The properties of alloy steel studied in this work are listed in **Table 2**.

FINITE ELEMNT MODELLING

Modeling 3D cutting process using finite element techniques is an area of ongoing research activity due to significant cost savings and offers insights into the process which are not easily measured in experiments, . In particular heat transfer and the modeling of cutting process requires careful consideration in any modeling activity. This paper presents approaches for modeling the turning process for four types of alloy steel. In this study, a Finite Element Analysis software Deform 3D is used to study the effects of cutting speed, feed rate, and type of alloy steel in temperature behavior. The work-piece is modeled as Elastic-plastic material to take thermal, elastic, plastic effect. Work-piece is represented by a liner model with different length for each condition.

The short material length was chosen to save computational time without compromising the model integrity as heat generation in machining is confined in small areas around the cutting zone.

The work-piece shape is constructed by the DEFORM machining module, and includes geometry created by a previous tool pass, including appropriate depth of cut and nose radius details. An unstructured tetrahedral finite element mesh was generated using DEFORM's automatic mesh generation system. Re-meshing parameters, including minimum element size, and parameters for adaptive mesh definition are set within the system. For these Procedures of the simulations, a minimum element size of 0.25 of the fed rate was specified. The total number of elements was 100000 to 130000 depending upon work-piece size. The Lagrangian calculation embeds a computational mesh in the material domain and solves for the position of the mesh at discrete points in time. An incremental Lagrangian formulation with an implicit integration method designed for large deformation simulations is used to simulate the cutting process. The solver used was the sparse matrix with a direct integration method, because the conjugate-gradient offers an improved computational speed but less stability in convergence.

RESULT AND DISCUSSION

A comparison between the constructed model presented in this work with experimental data and computed values of the average cutting temperature data using AdvantEde PL-TD FEM simulation predicted by(**Grzesik ,2008**) is presented in **Fig.(3)**. Taken same conditions used in this Reference .i.e. cutting speeds of (103.2, 206.4, 330 m/min), feed rate of 0.16 mm/rev and depth of cut of 2 mm with AISI 1045 work-piece material and ISO P20 uncoated carbide tool. Thermal properties (k, c_p, and   ) for tool material taken from Ref.(**Umbrello,2007**). Fig.(3) shows good agreement between experimental date of Ref.(**Grzesik , 2008**)and present FE model for the three selected cutting speeds with percentage error of (3.75, 7.03, and 2.616)% for speeds 103.2, 206.4, and 330 mm/min respectively.

Assuming that the cutting region apply as moving heat source, along the surface of the work-piece in the +y direction , see **Fig.(4)**, that means the maximum temperature absolutely lay near this region ,since maximum friction , interface pressure between tool and work-piece, and shear stress lay in this region. But it's behavior with time differs, in the early stage of the cutting process, only the heat transferred is absorbed, resulting a rapid increase in the local temperature, after that the heat transferred is partially absorbed to raise its enthalpy and is then partially diffused into the neighboring domain assume there is no convection under the tool because the solid surface of the work-piece is covered by the tool (just near cutting zone i.e zone of maximum temperature). That's mean maximum amount of heat will transfer by conduction to the work-piece and tool neglecting heat transfer by radiation. This results in a temporarily increase in the local temperature which then nearly approaches its final steady value, since the amount of work done on the workpiece is constant with fixed cutting velocity and feed rate, as shown in **Fig.(5)**.

Fig. (5) Shows temperature response for cutting AISI 1045, AISI 1030, AISI 4340 and AISI 4140 steel. It is disclosed that the temperature response is temporally and approximately exponential with fluctuations, the amplitude of the fluctuations differs for each other depending on the thermal properties and internal composition of each one (chromium, manganese, molybdenum, phosphorus, silicon and sulphur) specially the rate of (Sulphur) which increase machining capability then reducing shear effect , finally reducing the cutting temperature. The extent of temperature oscillations varies with the work materials which are most severe in cutting AISI 1030 then AISI 4140, AISI 4340 and AISI 1045 steel. These temperature fluctuations are caused by chip formation, which raises the local temperature upon contact with the tool material. The difference in the extent of temperature oscillations can be attributed to the differences in chip size during machining operations and the properties of the work-piece materials. The data drawn in **Fig (5)** can be fitted as a time polynomials (applies in the earlier stages till 3msec which gives steady state temperature) for each alloy at the different conditions can be arranged in **Table (3).**

It is clearly from **Fig.(5)** that steady state may reaches depending on the operating conditions ,it has an inversely proportion with operating conditions. Maximum time may need to reach steady

state starting 1.11msec for low conditions to 2.8 and 3msec for medium and high conditions respectively. Also these values differ from alloy to other that AISI 1045 need less time followed by AISI 4340, AISI 4140 and AISI 1030 to reach steady state.

Figs (6) and (7) depicts the effects of feed and cutting speed on the steady state temperature for the four alloys respectively at a constant depth of cut(1mm). They are essentially a plot of the temperature equation variation. For a constant cutting speed 53.4 m/min Fig**. (6)**, of V= 54.4m/min, all alloys have a sever increasing in temperature with increasing feed rate, since increase in feed rate lead to increasing the section of chip and consequently friction increases as reported by Shaw in (Jing, 2005).The sensibility to cutting process change with increasing feed rate differs from alloy to other depending to shearing force and machining capability for each one. AISI 1030 and AISI 4140 have higher cutting temperature curve than AISI 4340 and then AISI 1045 with increasing feed rate ,these arrange for the four alloys repeat for each cutting speed **Figs.(6)**,V=103.2 ,206.4 and 330 m/min, except the coincidence between AISI 1030 and AISI 4140 ,these appear coincides at cutting speed 53.4 m/min and any range of feed rate because of rapprochement in thermal properties **Fig.(6)** of V=53.4 m/min , then starting contrast between this alloys with increase cutting speed **Fig (6)** V=103.2 ,206.4 and 330 m/min ,for appearing the effect of chemical composition with increasing cutting temperature by increasing cutting speed.

The same tendency appears in **Fig. (7)**, for the effects of cutting speed on the steady-state temperature for all work-piece alloys. Except that the behavior for the steady state temperature looks less sharp and has exponential form even with low feed rate **Fig. (7)**, of V=53.4m/min). That's mean the liner trend caused by low cutting speed not feed. The same word may say for the behavior of AISI 4140 and AISI 1030, the congruity present only in low cutting speed region but not low feed. Also arrangement of alloys machining acceptability dos not effected, that's AISI 1045 then AISI 4340, AISI 4140 lastly AISI 1030. Temperature is closely connected to cutting speed, with increase of cutting speed friction increases; this induces an increase in temperature in the cutting zone.

Also the percentage of the number of nodes which have range of temperature with respect to total number could be calculated directly in 3D-DEFORM. So comparison made in **Fig.(8)** among alloys shows the range of temperatures distribution in each alloy for cutting speed 220.4 m/min ,feed rate =0.2 mm/rev and 1mm as a depth of cut. Percentage of nodes have ranges of maximum temperature covers minimum ratio of nodes number reach to (0.745, 0.836, 0.583, 0.613) % for AISI 1045, AISI 4340, AISI 4140 and AISI 1030 respectively.

CONCLUSIONS

 The following conclusions could be drawn from the results of present study:

1) Finite element method using DEFORM 3D program is found to be a successful technique to perform trend analysis to estimate cutting temperatures in metal cutting with respect to various combinations of design variables (metal cutting speed, feed rate and depth of cut).

2) Polynomial models of third, fourth and fifth degree are found to be adequately representing metal cutting temperature results with time applies in the earlier stages till 3msec to give steady state temperature for different operating conditions and for AISI 1045, AISI 4140,AISI 4340 and AISI 1030 alloys steel.

3) Steady state temperature may reach in time less than 3 msec depending on alloy steel properties and operating conditions.

4) All alloys have a sever increasing in steady state temperature with increasing feed rate, while it looks less sharp and has exponential form with increasing cutting speed .

5) A coincidence in steady state temperature curve between AISI 1030 and AISI 4140 appear at cutting speed 53.4 m/min and any range of feed rate, then starting contrast between this alloys with increase cutting speed .

6) Percentage of number of nodes which have range of temperature respect to total number for all alloys seems closely convergent but not the temperature which respected by this ranges.

REFRENSES

-Abhang, L. B. and Hameedullah M. , "Power Prediction Model for Turning EN-31 Steel Using Response Surface Methodology", Journal of Engineering Science and Technology Review ,3 (1), 116-122,2010.

- Abukhshim, N.A , Mativenga, P.T, Sheikh, M.A.," Heat generation and temperature prediction in metal cutting: A review and implications for high speed machining" ,International Journal of Machine Tools & Manufacture ,46,782–800, 2006.

- Abukhshim, N.A , Mativenga, P.T, Sheikh, M.A. ," Investigation of heat partition in high speed turning of high strength alloy steel, International Journal of Machine Tools & Manufacture", 45 , 1687–1695,2005.

- Derakhshan , E.D. and Akbari, A.A., "Experimental Investigation on the Effect of Workpiece Hardness and Cutting Speed on Surface Roughness in Hard Turning With CBN Tools", Proceedings of the World Congress on Engineering ,Vol II, July 1 - 3, 2009, London, U.K. WCE 2009.

- DEFORM-3D User manual Version6.1 ,18th oct. ,2007.

-Grzesik, W.," Composite layer-based analytical models for tool–chip interface temperatures in machining medium carbon steels with multi-layer coated cutting tools", Journal of Materials Processing Technology ,176 ,,102–110,2006.

 -Grzesik ,W. and Niesony, P.," FEM–based thermal modelling of the cutting process using power law temperature dependent concept", Archives of Materials Science and Engineering, Volume 29, Issue 2 February, Pages 105-108,2008.

-Haci Saglam, Faruk Unsacar, Suleyman Yaldiz, " Investigation of the effect   of rake angle and approaching angle on main cutting force and tool tip temperature", International Journal of Machine Tools & Manufacture 46, 132–141,2006.

-Jing Li, J.C.M. Li ," Temperature distribution in workpiece during scratching and grinding ",Materials Science and Engineering ,A 409 ,108–119,2005.

-Karpat Y.,and Özel T.," Process Simulations for 3-D Turning using Uniform and Variable Micro-   Geometry PcBN Tools".

-Özel T., Correia A.E. and Davim J.P. ,"Neural network process modelling for turning of steel parts using conventional and wiper inserts", Int. J. Materials and Product Technology, Vol. 35, Nos. 1/2, pp.246–258, 2009.

-Pradip Majumdar , Jayaramachandran R., Ganesan S.," Finite element analysis of temperature rise in metal cutting Processes",Applied Thermal Engineering, 25, 2152–2168, 2005.

-Rogério Fernandes Brito , Solidônio Rodrigues de Carvalho , Sandro Metrevelle Marcondes de Lima e Silva , João Roberto Ferreira ," Thermal analysis in coated cutting tools", International Communications in Heat and Mass Transfer 36 , 314–321,2009.

-Sutter G., Ranc N., "Temperature fields in a chip during high-speed orthogonal cutting—an experimental investigation", International Journal of Machine Tools & Manufacture 47, 1507–1517, 2007.

-Sarat Babu Singamneni ," A mixed solution for the three-dimensional temperature distribution in turning inserts using finite and boundary element techniques ",Journal of Materials Processing Technology ,166 ,98–106,2005.

-Umbrello D. , Filice L., Rizzuti S. , Micari F. , Settineri L., "On the effectiveness of Finite Element simulation of orthogonal cutting with particular reference to temperature prediction", Journal of Materials Processing Technology ,189, 284–291,2007.

-Vincent Dessoly , Shreyes N. Melkote and Christophe Lescalier," Modeling and verification of cutting tool temperatures in rotary tool turning of hardened steel", International Journal of Machine Tools & Manufacture, 44 ,1463–1470,2004.

www.Mat-lab.com

-Yang W.H and Tarng Y.S.," Design optimization of cutting parameters for turning operations based on the Taguchi method", Journal of Materials Processing Technology, 84, 122–129, 1998.

Table (1) summary of cutting conditions

Flat insert	TNMA 332
Rake angle	-5
Clearance angle	-5
V	53.4 ,103.2 , 206.4, 330 m/min
F	0.05, 0.15, 0.2 mm/rev
t1	1 mm
Workpiece	AISI 1045, AISI 1030 ,AISI 4340, AISI 4140 STEEL
Coulomb friction coefficient	0.5
Type of cutting tool	WC uncouted
tool thermal conductivity (k)	59 N/sec/K
Tool heat capacity (c_p)	15 N/mm^2/K
tool density ( )	15800 kg/m³

Table (2) Physical properties of workpiece alloys (www.Mat lab .com) and (DEFORM-3D manual,2007)

Property	AISI 1030	AISI 1045	AISI 4140	AISI 4340
Thermal conductivity (k)	from 46.8 (at 20 °C) to 31.74 (at 700 °C) to25.09 at (1000°C)	from 41.9(at 20 °C) to22.5 at (T>850 °C)	From 41.9(at 20 °C) to22.5 at(T>850°C)	41.7(at 20 °C) to43.4 (at 100°C)to 34.1^{o}C at (T 600°C)
heat capacity (c_p) N/mm^2/K	from 3.35 (at 20 °C) to 7.2 (at 1000 °C)	3.6(at 20 °C) 6.1(T 600 °C	From 3.6(at 20 °C) to6.1(T 600 °C)	From 3.6(at 20 °C) to 6.1(T 600 °C
density ( ) kg/m³	7850	7860	7830	7850
Poisson's ratio	0.3	0.3	0.3	0.3
Young's modulus (E) (Gpa)	from 212 (at 20 °C) to 130 (at 900 °C)			

Table (3) Time polynomials for each alloy steel at the different conditions

Type of Alloy steel	*Operating Condition	Formula
AISI 1045	High	$T=3*10^{11}t^3-8*10^8t^2+9.25*10^5t+T_i$
	Medium	$T=-4*10^{13}t^4+3*10^{11}t-7*10^8t^2+9*10^5t+T_i$
	Low	$T=9*10^{10}t^3-3*10^8t^2+4.5*10^5t+T_i$
AISI 4340	High	$T=-8*10^{14}t^4+3*10^{12}t^3-4*10^9t^2+2*10^6t+T_i$
	Medium	$T=9*10^{16}t^5-5*10^{14}t^4\_+10^{12}t^3-2*10^9t^2+10^6t+ T_i$
	Low	$T=-2*10^{13}t^4+2*10^{11}t-5*10^8t^2+7*10^5t+T_i$
AISI 4140	High	$T=10^{18}t^5-4*10^{15}t+7*10^{12} t^3-6*10^9 t^2+3*10^6+ T_i$
	Medium	$T=7*10^{16}t^5-4*10^{14}t^4+10^{12}t^3-2*10^4t^2+10^6t +T_i$
	Low	$T=-3*10^{13}t^4+3*10^{11}t-9*10^8t^2+9.12*10^5t+T_i$
AISI 1030	High	$T=7*10^{17}t^5-3*10^{15}t^4+6*10^{12}t^3-6*10^9t^2+3*10^6t+T_i$
	Medium	$T=10^{17}t^5-6*10^{14}t^4+2*10^{12}t^3-2*10^9t^2+2*10^6t+ T_i$
	Low	$T=-5*10^{19}t^6 +6*10^{17}t^5-2*10^{15}t^4+4*10^{12}t^3-4*10^9t^2 +2*10^6t +T_i$

* high operating conditions   f=0.2 mm/rev, v=330 m/min ;
medium operating conditions f=0.15mm/rev, v=103.2 m/min;
low operating conditions   f=0.05mm/rev, v=53.4 m/min.
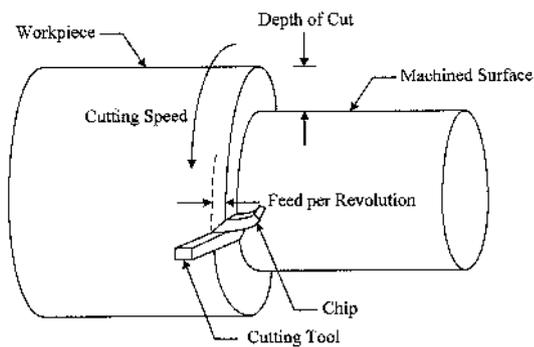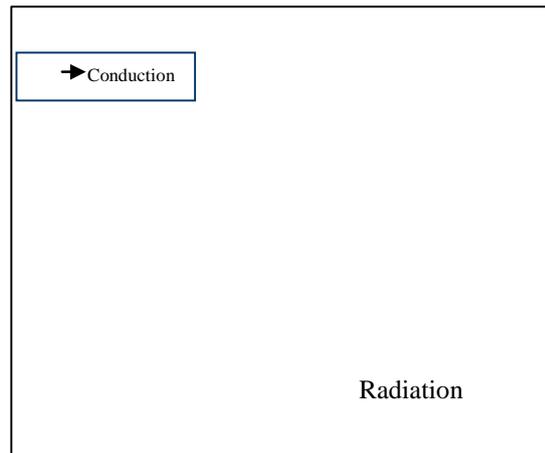
(a)   (b)

Fig.(1) Turning process (a) Basic cutting parameters (**Yang ,1998**).
(b)Thermal fields (Abukhshim, 2006).
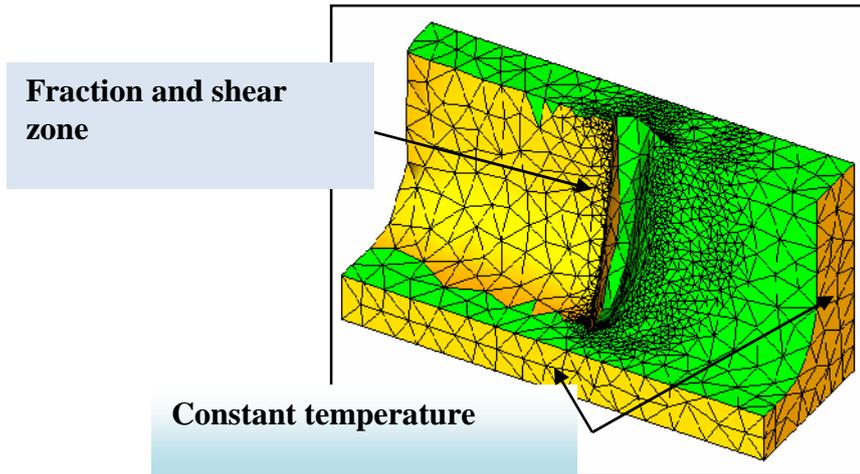
**Fig. (2)** Boundary conditions on the workpiece.
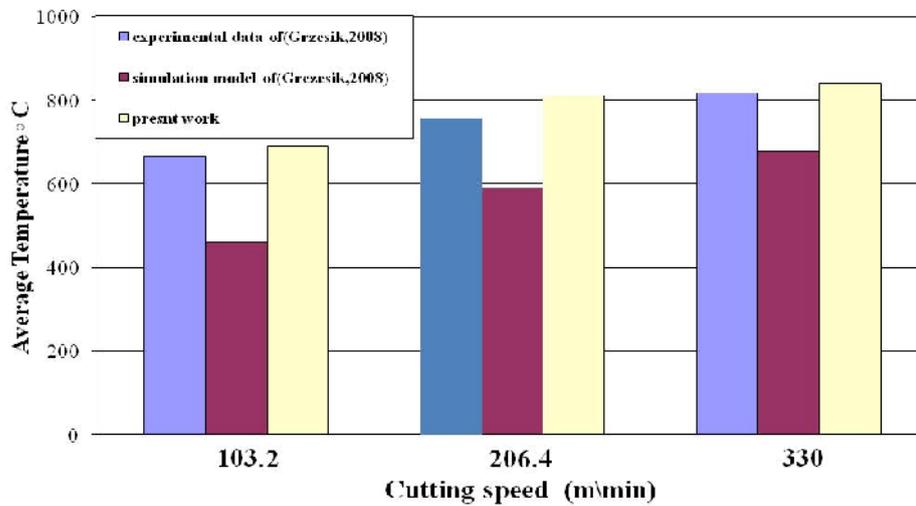
Fig.(3) Comparsion of the experimental cutting Temperature and FEM simulated values of (Grzesik,2008) with FEM simulation model in presnt work
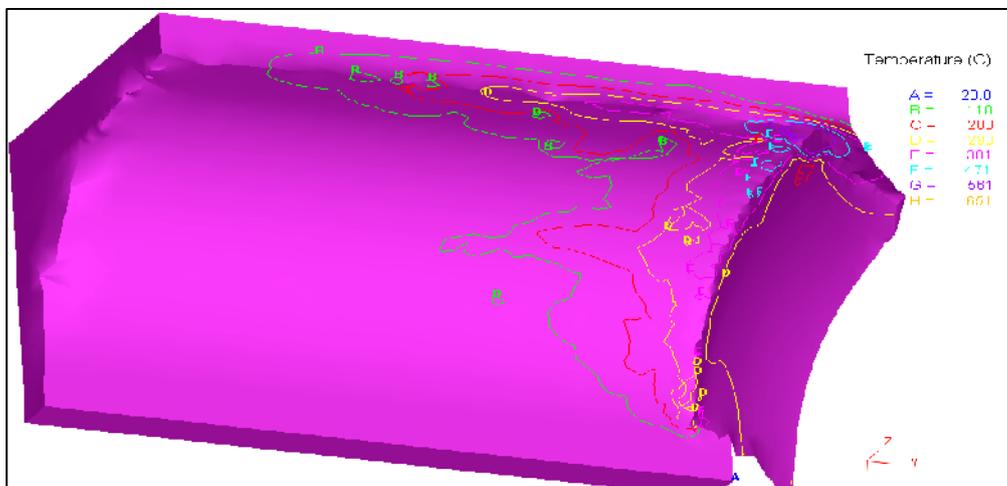

Fig.(4) Temperature distribution on cutting surface of   workpiece of AISI 1030,V=330m/min, f=0.05rev/min, d=1mm after 0.000364sec from starting **cutting.**
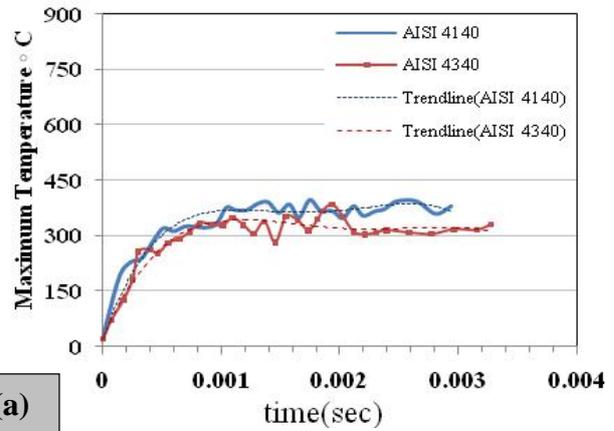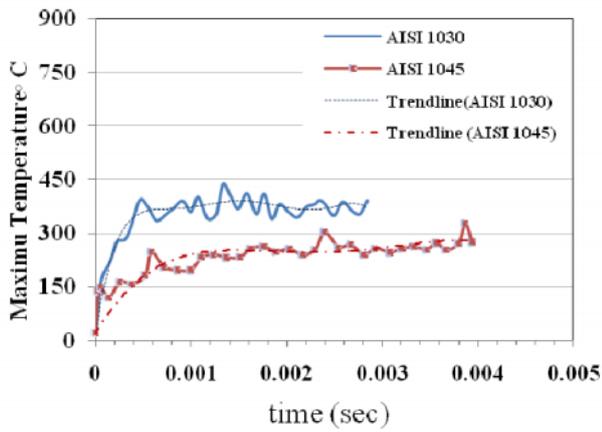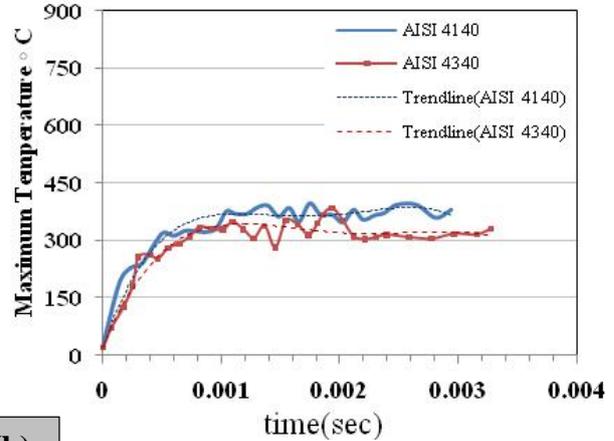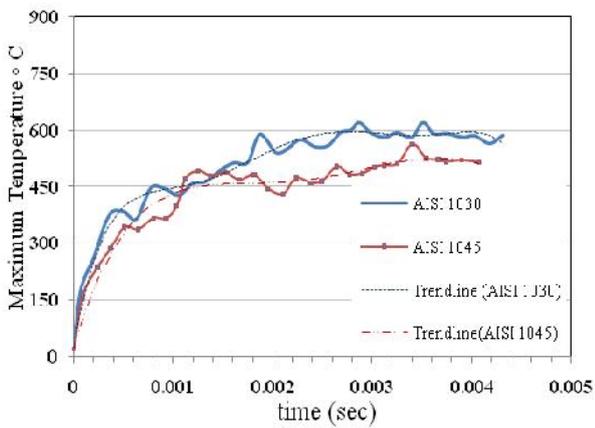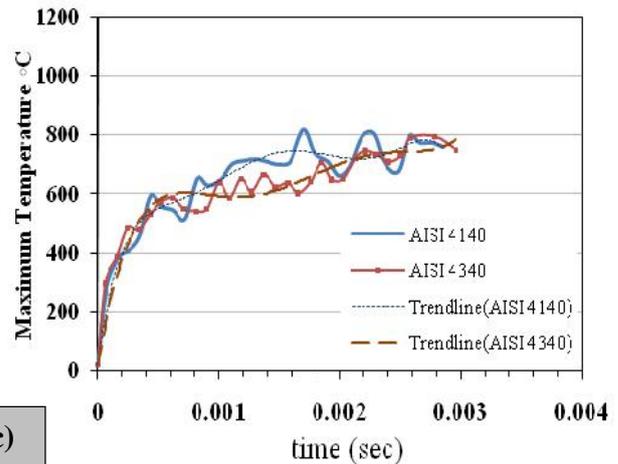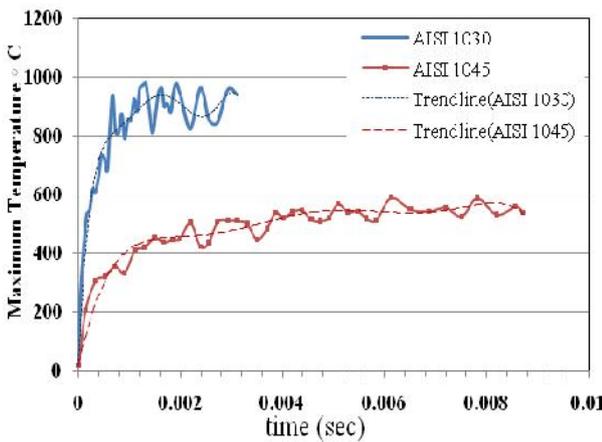
Fig. (5) Comparison of temperature response in early and beginning of steady stages for workpieces used;
(a) at low operating conditions f=0.05mm/rev, v=53.4 m/min ;
(b) at medium operating conditions f=0.15mm/rev, v=103.2 m/min;
(c) at high operating conditions f=0.2 mm/rev, v=330 m/min.
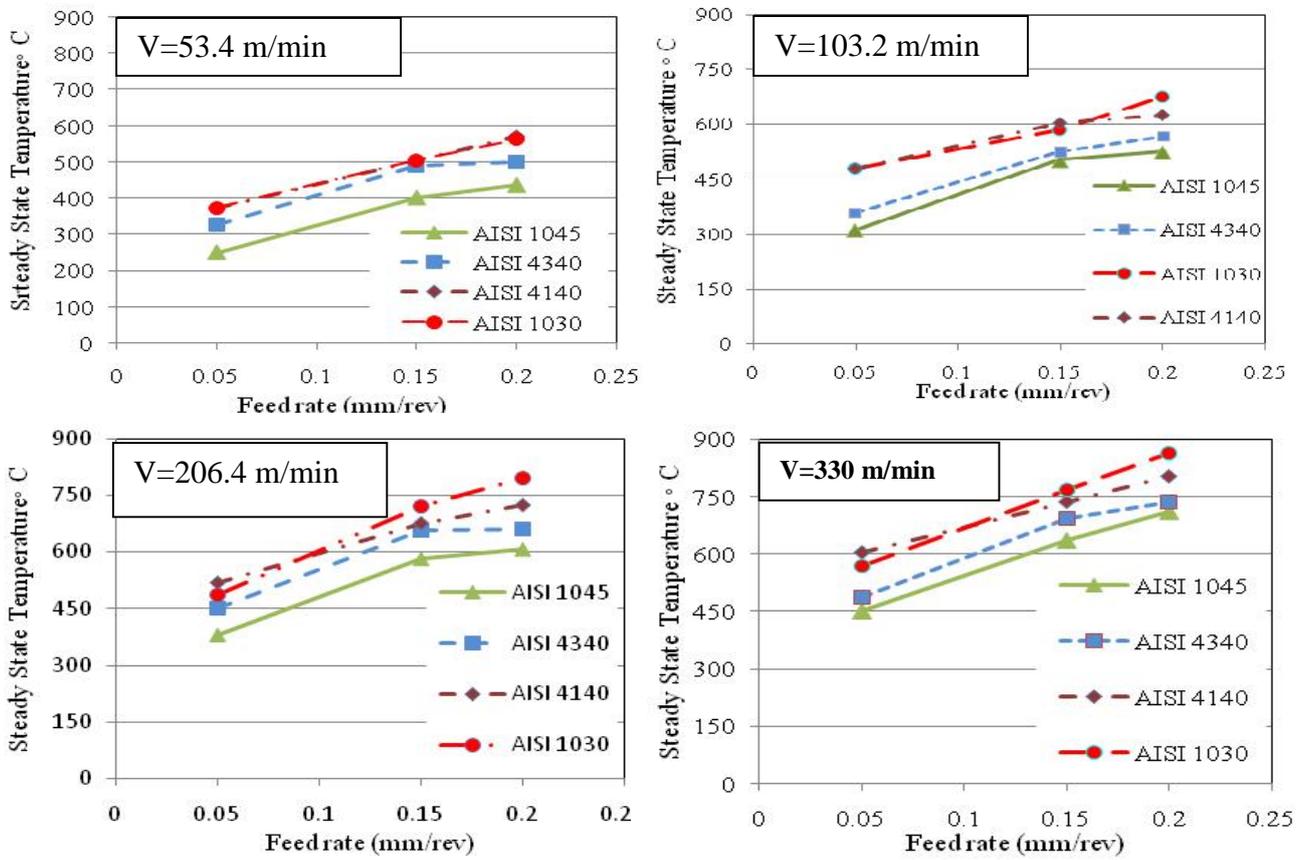
Fig.(6) Effects of feed rate on steady-state temperature in the work materials at different cutting speed
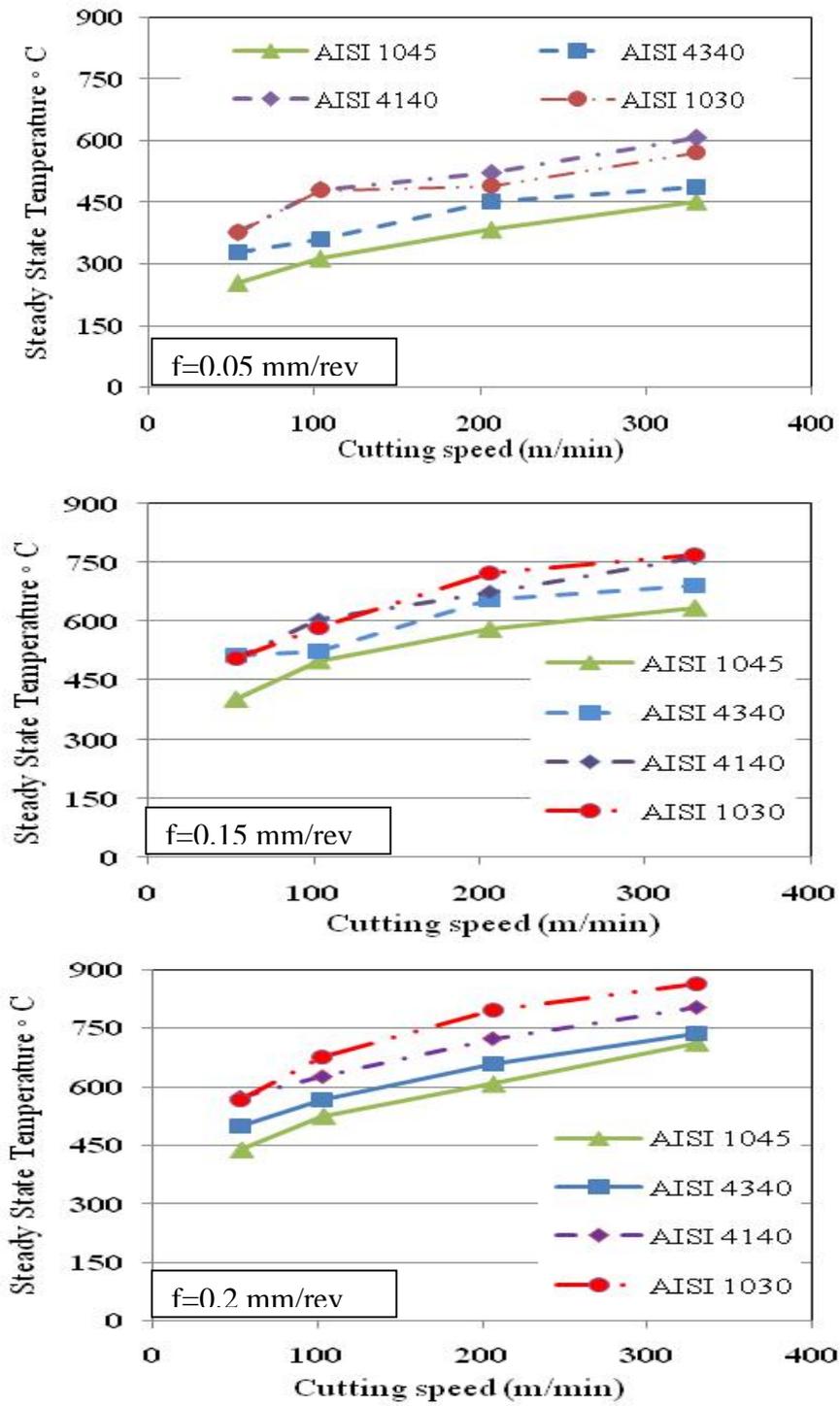
Fig. (7) Effects of cutting speed on steady-state temperature in the work materials for different feeds

(a) AISI 1045

(b)AISI 4340


(c) AISI 4140

(d)AISI 1030
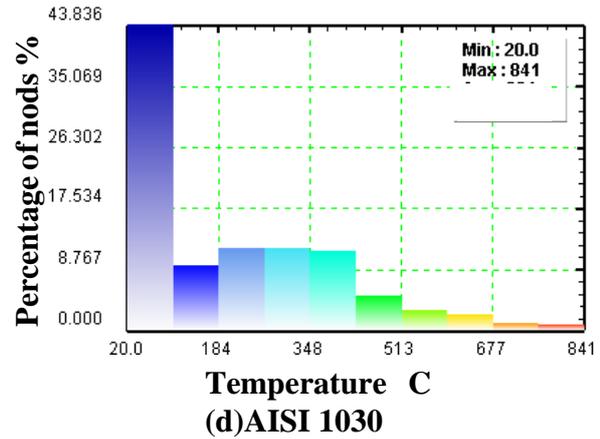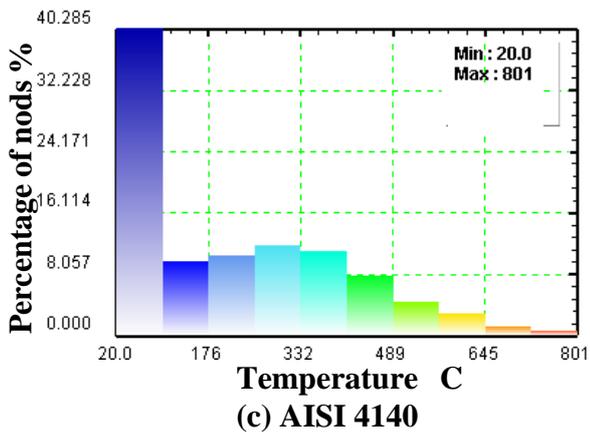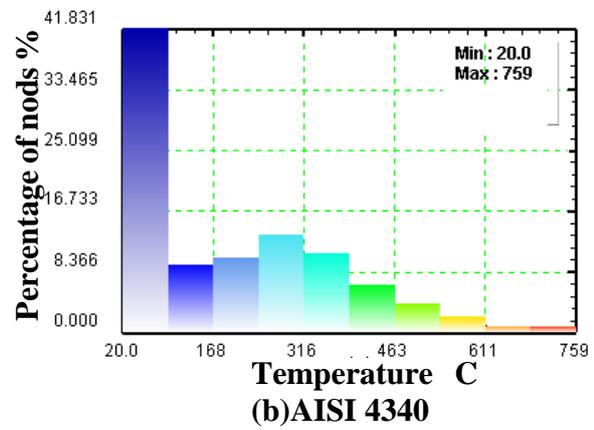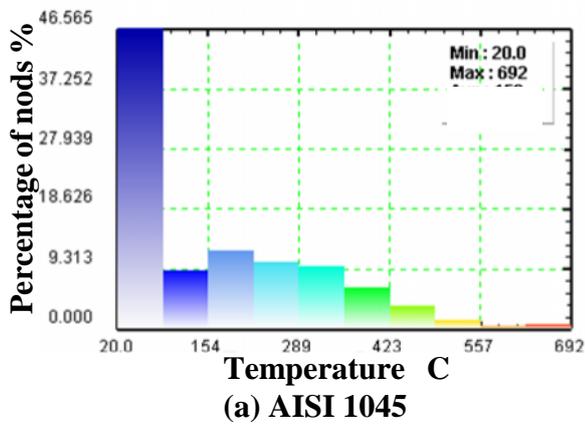
Fig. (8) Histogram shows the percentage of nodes with its temperature range for workpiece of 8mm length after cutting time 0.00181 sec.